Check for updates

Geophysical Research Letters

RESEARCH LETTER
10.1029/2022GL097903

Equatorial Origin of the Observed Tropical Pacific Quasi-Decadal Variability From ENSO Nonlinearity

Chao Liu[1], Wenjun Zhang[1], Fei-Fei Jin[2], Malte F. Stuecker[3], and Licheng Geng[2]

[1]CIC-FEMD/ILCEC, Key Laboratory of Meteorological Disaster of Ministry of Education (KLME), Nanjing University of Information Science and Technology, Nanjing, China, [2]Department of Atmospheric Sciences, School of Ocean and Earth Science and Technology (SOEST), University of Hawai'i at Mānoa, Honolulu, HI, USA, [3]Department of Oceanography & International Pacific Research Center (IPRC), School of Ocean and Earth Science and Technology (SOEST), University of Hawai'i at Mānoa, Honolulu, HI, USA

Key Points:

- Observations show that CP-ENSO-like quasi-decadal variability originates in the equatorial Pacific and extends to the off-equatorial region
- The equatorial ocean heat content and sea surface temperature are in phase on quasi-decadal timescales, whereas they are in quadrature for interannual ENSO
- Equatorial nonlinear dynamical heating is proposed as the dynamical origin of the quasi-decadal variability

Supporting Information:

Supporting Information may be found in the online version of this article.

Correspondence to:

W. Zhang,
zhangwj@nuist.edu.cn

Citation:

Liu, C., Zhang, W., Jin, F.-F., Stuecker, M. F., & Geng, L. (2022). Equatorial origin of the observed tropical Pacific quasi-decadal variability from ENSO nonlinearity. *Geophysical Research Letters*, *49*, e2022GL097903. https://doi.org/10.1029/2022GL097903

Received 15 JAN 2022
Accepted 7 MAY 2022

Abstract Quasi-decadal (QD) climate variability is detected in the tropical Pacific based on the recent 70 years of observations. This QD variability is identified in equatorial sea surface temperatures (SSTs), the pattern of which resembles the Central Pacific (CP) El Niño-Southern Oscillation (ENSO) but extends further meridionally to the northeastern subtropical Pacific. Whereas equatorial upper-ocean heat content and SSTs are in quadrature for ENSO, these two quantities are almost in phase on the QD timescale. Further analysis shows that nonlinear dynamical heating, primarily originating from strong El Niño events, tends to lead QD SSTs by a quarter of its dominant period (approximately 30 months) and shapes the dominant QD periodicity in observations. Our results suggest that the observed QD variability largely originates from ENSO nonlinearity and thus is fundamentally different from ENSO's oscillatory nature.

Plain Language Summary The climate variability of the tropical Pacific atmosphere-ocean system profoundly influences the global weather and climate patterns on a wide range of temporal scales. The dynamical understanding of interannual climate variability dominated by the well-known El Niño-Southern Oscillation (ENSO) phenomena has established a promising way for the operational seasonal to interannual climate prediction. So far, nevertheless, there is still a lack of consensus for the understanding of tropical Pacific decadal climate variability despite the increasing desire for climatic information on longer timescales. In this article, we illustrate the evolution features and possible governing mechanisms of a prominent quasi-decadal (QD) variability in the tropical Pacific with the utilization of an advanced spectrum approach and reliable observational data sets. The results show that this QD variability that makes up a substantial portion of tropical Pacific low-frequency variance is largely equatorial originated from the ENSO nonlinearity, which is dynamically different from the oscillatory nature of the ENSO phenomenon. Our study has important implications for the decadal climate prediction and improving the representations of tropical Pacific decadal variability in climate models.

1. Introduction

The tropical Pacific ocean and atmosphere exhibit pronounced interannual and low-frequency climate variability. Being the leading interannual climate mode, the El Niño-Southern Oscillation (ENSO) phenomenon has been extensively studied over the past several decades, laying the foundation for operational predictions of seasonal to interannual climate variations (e.g., Bjerknes, 1969; McPhaden et al., 2010; Meehl et al., 2021; Neelin et al., 1998). However, there is still a lack of consensus regarding the dynamic nature of Pacific low-frequency variability beyond ENSO timescales (e.g., Z. Liu, 2012; Z. Liu & Di Lorenzo, 2018; Newman et al., 2016; Power et al., 2021; Stuecker, 2018). In particular, some studies argued that a statistically significant narrowband quasi-decadal (QD; also simply referred to ''decadal'' in some previous studies; here we add "quasi" to distinguish it from longer multi-decadal timescales) spectral peak (~10 yr periodicity) above a red noise background spectrum can be detected in sea surface temperature (SST) and sea level pressure fields across the Pacific basin (e.g., Brassington, 1997; Tourre et al., 2001). Later studies showed that QD variability is manifested by a basin-wide spatial structure reminiscent of the Central Pacific (CP) ENSO and its associated atmospheric teleconnections (e.g., Lyu et al., 2017; Ren et al., 2013; Stuecker, 2018; Sullivan et al., 2016). Similar QD variability also exists in many other statistical climate modes, such as the Pacific meridional mode (PMM), the North Pacific Gyre Oscillation (NPGO), the Pacific Decadal Oscillation (PDO), and the Interdecadal Pacific Oscillation as

© 2022. American Geophysical Union. All Rights Reserved.

19448007, 2022, 10, Downloaded from https://agupubs.onlinelibrary.wiley.com/doi/10.1029/2022GL097903 by CochraneChina, Wiley Online Library on [13/11/2026]. See the Terms and Conditions (https://onlinelibrary.wiley.com/terms-and-conditions) on Wiley Online Library for rules of use; OA articles are governed by the applicable Creative Commons License

evidenced by their respective spectral features (e.g., Chiang & Vimont, 2004; Di Lorenzo et al., 2010, 2008; C. Liu et al., 2019; Lyu et al., 2017; Power et al., 1999, 2021; Stuecker, 2018). Especially, one recent study argued that the SST forcing in the equatorial central Pacific can generate PMM-like off-equatorial SST anomalies by altering the extratropical atmospheric circulation and associated surface heat fluxes (Stuecker, 2018). Tropical Pacific QD variability also exerts a strong influence on decadal variations of precipitation over southern China and the United States, as well as tropical cyclone activity in the western North Pacific (Kao et al., 2018; C. Liu et al., 2019; S.-Y. Wang et al., 2009, 2010, 2011, 2014).

Considering the importance of tropical Pacific QD variability to climate in the surrounding regions, a comprehensive understanding of its dynamical mechanisms is warranted. Historically, a substantial body of hypotheses has been put forward to explain the spatial and temporal features of tropical Pacific decadal variability. To first order, decadal variability can be conceptualized as a reddening ocean process driven by white uncorrelated atmospheric forcing. The long damping timescale due to the large ocean heat capacity effectively enhances variance at low frequencies but with no preferred spectral peaks (Frankignoul & Hasselmann, 1977; Hasselmann, 1976). On this basis, it was found that an ENSO-like SST pattern (albeit with much-reduced amplitude) and corresponding atmospheric circulation anomalies can be somewhat realistically reproduced with only a thermodynamic slab ocean coupled to a general circulation atmosphere model (Clement et al., 2011). In their model configuration, the cloud shortwave radiative feedback in the equatorial Pacific and the off-equatorial trade wind-evaporation-SST (WES) feedback plays important roles in the ENSO-like SST pattern formation. However, the absence of dynamic coupling with the ocean prevents this "thermodynamic ENSO" from reaching realistic SST amplitudes as seen in the observations. Ocean dynamical processes are often invoked to explain a preferred timescale of decadal SST variability. Theoretical studies have shown that there exists a family of basin-scale free eigenmodes in the context of linear ocean dynamics with a first baroclinic mode vertical structure (Jin, 2001; Z. Liu, 2002). These free oceanic eigenmodes essentially reflect the collective roles of oceanic Rossby waves at different latitudes that have different intrinsic time periodicities ranging from a few years (close to the equator) to several decades (far from the equator). Specific free decadal eigenmodes of ocean dynamics can be energized through either temporal stochastic forcing with favorable wind patterns or ocean-atmosphere coupled dynamics. For example, it has been hypothesized that tropical Pacific QD variability can be dynamically regarded as a recharge-discharge oscillator or a delayed oscillator through a dynamical coupling between tropical SST and subtropical ocean Rossby wave dynamics resulting in slow variations of Sverdrup transport (X. Wang et al., 2003a, 2003b; White et al., 2003). These oscillatory dynamics proposed to explain tropical SST variability on decadal timescales are very similar to those on interannual timescales for ENSO, except that the latter emphasizes ocean memory from equatorial wave dynamics (e.g., Jin, 1997a, 1997b; Suarez & Schopf, 1988). Besides the first baroclinic oceanic Rossby wave, it has also been hypothesized that decadal ocean memory can arise from higher-order vertical baroclinic modes in the equatorial Pacific based on one model simulation (Liu, 2002). Alternative perspectives of oceanic tunnels (i.e., the Subtropical Cells, STCs) are also provided to link the extra-tropical and tropical climates on decadal timescales (e.g., Capotondi et al., 2005; Chang et al., 2006; Gu & Philander, 1997; Kleeman et al., 1999; Lohmann & Latif, 2005; Nonaka et al., 2002; Power et al., 2021; Stuecker et al., 2020; Zeller et al., 2020; Zhang & McPhaden, 2006). Due to the blocking effect of the oceanic potential vorticity barrier induced by the Intertropical Convergence Zone in the North Pacific, the mechanism of the meridional oceanic circulation is argued to be more viable in the South Pacific (e.g., Luo et al., 2003; Luo & Yamagata, 2001; Schneider et al., 1999).

Apart from linear oscillatory theories, external and internal forcings can also drive tropical Pacific decadal variability. On the one hand, a few studies presume QD variability to be (at least partially) externally forced by solar activity variability considering their similar periodicities (e.g., Chunhan et al., 2021; Liang et al., 2021; Meehl et al., 2008, 2009; White & Liu, 2008a, 2008b). However, these results are highly model-dependent. On the other hand, ENSO can rectify onto the tropical Pacific mean state and contribute to its decadal variability (e.g., Choi et al., 2011, 2013; Hayashi & Jin, 2017; Hayashi et al., 2020; Kim & Kug, 2020; Ogata et al., 2013; Rodgers et al., 2004; D. Z. Sun et al., 2014; F. Sun & Yu, 2009). For example, the ENSO-induced nonlinear dynamical heating (NDH), especially pronounced during strong El Niño events, tends to be positive in the equatorial eastern Pacific for both El Niño and La Niña events and can thereby cause the asymmetry of ENSO intensity (An & Jin, 2004; Jin et al., 2003). The relevant ENSO residuals usually exhibit low-frequency changes, varying from one decade to another. While most previous studies focus on the time-mean rectification effect over a particular period, its connections with the observed decadal variability received less attention.

19448007, 2022, 10, Downloaded from https://agupubs.onlinelibrary.wiley.com/doi/10.1029/2022GL097903 by CochraneChina, Wiley Online Library on [13/11/2026]. See the Terms and Conditions (https://onlinelibrary.wiley.com/terms-and-conditions) on Wiley Online Library for rules of use; OA articles are governed by the applicable Creative Commons License

Despite numerous mechanisms postulated, no consensus has been reached for the underlying mechanisms of tropical Pacific QD variability so far (e.g., Power et al., 2021). Since the 1950s, after which observations of relatively good quality become available, QD variability has experienced about seven "cycles", allowing a chance to further investigate its possible mechanisms. In this study, we combine spectral and heat budget analyses to investigate tropical Pacific QD temporal and spatial features. We find that the QD signal largely originated from the equatorial central Pacific with ENSO-related NDH playing a key role in its genesis.

2. Data and Methodology

2.1. Data Set

The primary data sets used in this study are the Extended Reconstructed Sea Surface Temperature, version 5 (ERSSTv5) from the National Oceanic and Atmospheric Administration (Huang et al., 2017), as well as the ocean reanalysis from the German contribution to the Estimating the Circulation and Climate of the Ocean project, version 3 (GECCO3; Köhl, 2020). We also use other ocean reanalysis products and found similar results (see details in our main text). Reanalysis surface turbulent heat fluxes used in the mixed-layer heat budget analysis were obtained from the fifth reanalysis product of the European Center for Medium-Range Weather Forecast (ERA5; Hersbach et al., 2020). The analysis period is from 1950 to 2020. All variables were linearly interpolated onto a common grid with a $1^\circ \times 1^\circ$ horizontal spatial resolution and a 10 m vertical resolution in the upper ocean (down to 350 m depth). Anomalies were calculated relative to the climatology of the whole period and were linearly detrended. To isolate variability on QD timescale, an 8–20-year bandpass Lanczos filter was used (Duchon, 1979).

2.2. Methodology

2.2.1. Mixed-Layer Heat Budget

To quantify the contributions of different oceanic and atmospheric processes to observed tropical Pacific decadal variability, an ocean mixed layer heat budget analysis in partial flux form is utilized (An et al., 1999):

$$\frac{\partial T}{\partial t} = \frac{Q_{net}}{\rho C_p H} - \left(\frac{\partial \left(\overline{u}T\right)}{\partial x} + \frac{\partial \left(\overline{v}T\right)}{\partial y} \right) + \frac{\overline{w}T_H}{H} - \left(u\frac{\partial \overline{T}}{\partial x} + v\frac{\partial \overline{T}}{\partial y} + w\frac{\partial \overline{T}}{\partial z} \right) - \left(u\frac{\partial T}{\partial x} + v\frac{\partial T}{\partial y} + w\frac{\partial T}{\partial z} \right) \quad (1)$$

The variables T, u, and v denote the anomalous ocean temperature, zonal, and meridional ocean currents velocities averaged in the mixed layer, respectively. T_H and w represent the ocean temperature anomalies and vertical current velocities at the bottom of the mixed layer, while Q_{net} is the net anomalous heat flux into the ocean at the sea surface. Variables with an over-bar indicate climatological mean states, $\rho = 1{,}022$ kg/m^3 is the density of seawater, $H = 50$ m is the mixed layer depth, and $C_p = 4{,}000$ J/(kg K) is the heat capacity of seawater. The grouped five terms on the right-hand side represent thermal damping, dynamical damping by horizontal mean circulation, thermocline feedback, advective feedbacks in three directions, and NDH, respectively.

2.2.2. Multitaper Frequency-Domain Singular Value Decomposition (MTM-SVD)

Following previous studies, we here utilize the well-established MTM-SVD method to explore the observational features of the tropical Pacific decadal variability. The MTM-SVD is a multivariate signal processing method well suited for detecting narrowband spatiotemporal signals embedded in a red noise background (Mann & Park, 1994, 1999). It has been successfully applied to many research topics, such as the recent findings on the Atlantic multidecadal oscillation origins (Mann et al., 2021, 2020). A summary of this method is available in Text S1 in Supporting Information S1, and more details can be found in a review article by Mann and Park (1999).

3. Observational Features of Tropical Pacific QD Variability

Figure 1a shows the local fraction variance (LFV) spectrum for joint normalized raw oceanic fields over the tropical Pacific region (30°S–30°N, 100°E–80°W). Considering the sea surface height (SSH) is more representative of decadal information than the thermocline depth (isotherm 18°C; D18) around the equatorial central Pacific (Figure S1 in Supporting Information S1; Zhao et al., 2021), we here chose SSH as a dynamical field for analyses,

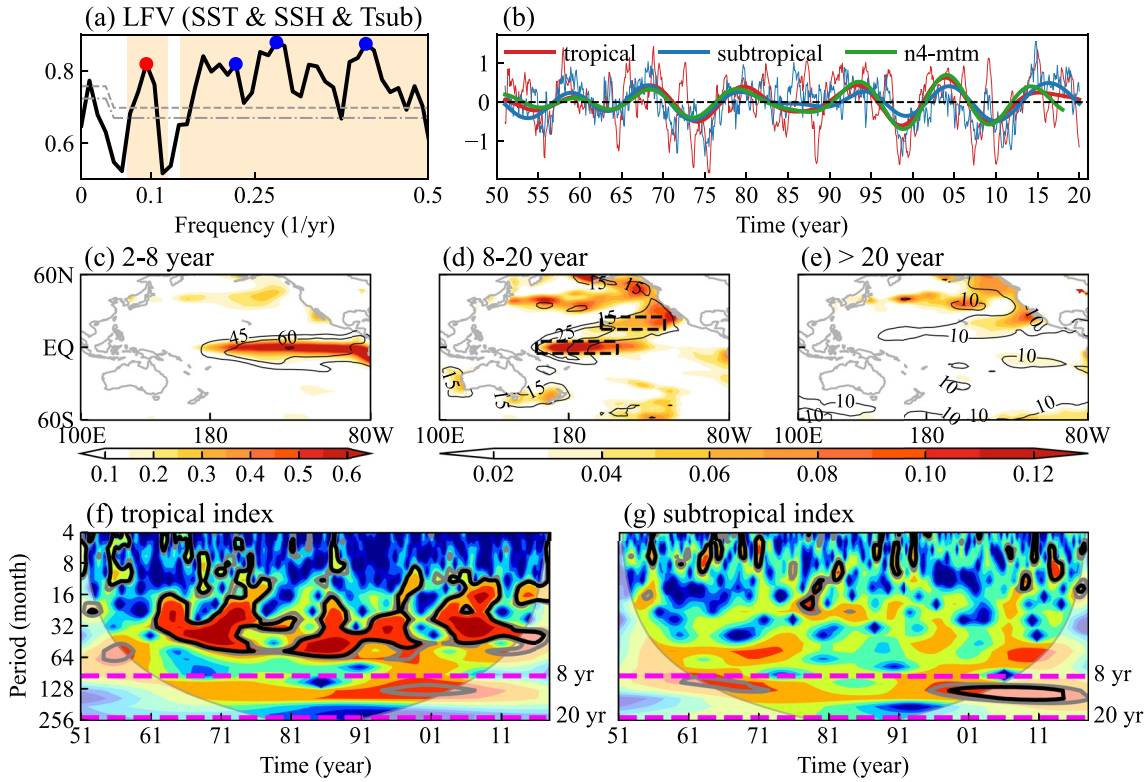


Figure 1. (a) Local fractional variance (LFV) spectrum for the combined tropical Pacific (30°S–30°N, 100°E–80°W) sea surface temperature (SST), sea surface height (SSH), and equatorial cross-section of subsurface temperature in the upper ocean (~350 m). The horizontal two dashed lines denote the corresponding 90% and 95% confidence levels based on the bootstrap method. (b) The time evolutions of Niño4 (thin red) and subtropical (thin blue) SST indices, as defined by dashed boxes in (d). Their 8–20 yr bandpass filtered components (thick), as well as the reconstructed Niño4 index (green) using the MTM-SVD method on a decadal timescale (period = ~10.7 yr; the red dot in (a)), are superimposed. Spatial distribution of the SST anomalies variance (shading, $°C^2$) and corresponding variance ratio (contours, %) on (c) interannual, (d) quasi-decadal, and (e) longer timescales. Bias-rectified wavelet power spectra of normalized SST indices in the indicated (f) Niño4 and (g) subtropical regions. Regions enclosed by gray and black contours indicate statistically significant variability at the 90% and 95% confidence levels when tested against an AR(1) null hypothesis. The parabola regions indicate the "cone of influence", where edge effects become important.

in combination with SST and equatorial subsurface ocean temperature. The result shows that Pacific climate variability exhibits prominent multiple-timescale features. These spectral results are rather robust to changes in the domain of analysis, the combinations of physical fields, the study period, and different data sources (Figure S2 in Supporting Information S1; Balmaseda et al., 2012; Carton et al., 2018; Zuo et al., 2019). Statistically significant LFV peaks on broad interannual timescales (e.g., 2–7 yr) largely reflect the well-known ENSO phenomenon as evidenced by the spatial pattern of the SST variance map (Figure 1c). Being the most energetic climate mode on interannual timescales, the ENSO-associated SST variability takes up around 60% of the total variance with its action center located in the equatorial central to eastern Pacific. In addition to the ENSO signal on interannual timescales, two additional significant peaks on longer timescales are detected. The first peak mainly represents the secular trend as it lies within one bandwidth (twice of the minimum resolvable frequency in this study) of zero frequency, which is not our focus here. The other peak is a narrow-band QD signal (period~10.7 yr), suggesting the potential existence of a spatially coherent oscillatory mode on this timescale. The corresponding variance of the detrended SST anomalies within the 8–20 yr period band exhibits a basin-scale structure reminiscent of the CP-ENSO and/or PMM (Stuecker, 2018) with large spatial loadings in the equatorial central Pacific, the subtropical northeast Pacific, and high latitude coastal regions of North America. The fraction of explained SST variance by QD variability is generally larger than 15% and even higher than 25% around the tropical central Pacific (Figure 1d). In comparison, the SST variance on timescales longer than 20 yr is less pronounced and mostly confined to the extratropical North Pacific (Figure 1e). Very similar results are obtained using other SST data sets (Figure S3 in Supporting Information S1; Ishii et al., 2005; Kennedy et al., 2011; Rayner et al., 2003). Based on the SST variance map, we choose SST indices over the traditional Niño4 (5°S–5°N, 160°E–150°W) and the subtropical northeast Pacific (15°N–25°N, 120°–160°W) regions to examine the temporal and spectral features

19448007, 2022, 10, Downloaded from https://agupubs.onlinelibrary.wiley.com/doi/10.1029/2022GL097903 by CochraneChina, Wiley Online Library on [13/11/2026]. See the Terms and Conditions (https://onlinelibrary.wiley.com/terms-and-conditions) on Wiley Online Library for rules of use; OA articles are governed by the applicable Creative Commons License

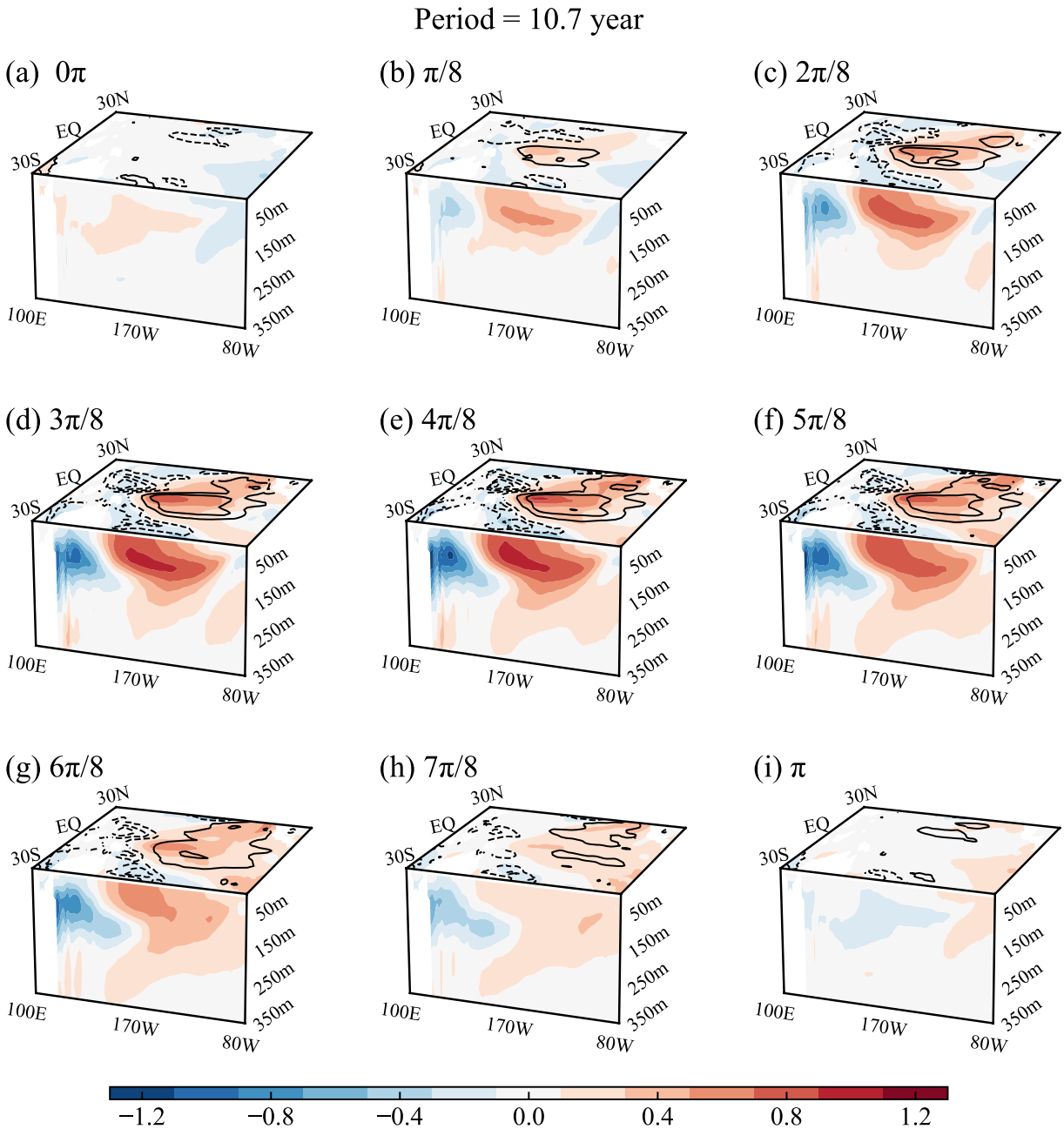


Figure 2. Phase evolution of tropical Pacific sea surface temperature (SST; shading, °C), sea surface height (SSH; contours, cm), and equatorial subsurface temperature (shading, °C) anomalies on quasi-decadal (QD) timescales (period = ~10.7 yr in the MTM-SVD analysis). The contour interval is 1.5 cm and the zero isolines are omitted.

of QD variability. These two indices are highly correlated ($R = 0.87$; Figure 1b) on the QD timescale. Similar QD variability can also be reconstructed using the MTM-SVD method (Figure 1b). However, the distinguishable QD variability is somewhat intermittent in terms of wavelet power and its statistical significance against an AR(1) null hypothesis (Figures 1f and 1g). There is only a marginally significant center around the 2000s on the QD timescale for both indices. While different statistical methods reveal a consensus phenomenon of distinguishable QD variability in observations (e.g., Lyu et al., 2017; Sullivan et al., 2016), its periodic behavior is most apparent in the recent two decades and may not necessarily reflect a natural oscillatory signal like ENSO.

Figure 2 shows the reconstructed phase evolution of the QD variability based on the MTM-SVD method. The three-dimensional structure of the QD variability generally resembles that for ENSO (Figures S4–S6 in

19448007, 2022, 10, Downloaded from https://agupubs.onlinelibrary.wiley.com/doi/10.1029/2022GL097903 by CochraneChina, Wiley Online Library on [13/11/2026]. See the Terms and Conditions (https://onlinelibrary.wiley.com/terms-and-conditions) on Wiley Online Library for rules of use; OA articles are governed by the applicable Creative Commons License

19448007, 2022, 10, Downloaded from https://agupubs.onlinelibrary.wiley.com/doi/10.1029/2022GL097903 by CochraneChina, Wiley Online Library on [13/11/2026]. See the Terms and Conditions (https://onlinelibrary.wiley.com/terms-and-conditions) on Wiley Online Library for rules of use; OA articles are governed by the applicable Creative Commons License

Supporting Information S1), especially around its mature phase, including the ENSO-like spatial pattern in SST, the zonal dipole contrast of the equatorial subsurface temperature as well as its surface expressions in SSH. Specifically, tropical Pacific decadal variability first emerges in the equatorial central Pacific and then spreads toward the subtropical regions, reflecting its equatorial origin. This propagating feature is supported by the cross-correlation analysis between tropical and subtropical SST and SSH variabilities, which is also evident in other data sets (Figure S7 in Supporting Information S1). The observational pattern evolution shown here is consistent with model results of one previous study, showing that a prescribed SST forcing in the tropical central Pacific alone can generate PMM-like subtropical SST anomalies (Stuecker, 2018). Despite the highly similar spatial structures and phase evolutions, there exists one fundamental difference between the QD variability and the interannual ENSO phenomenon around the transition phase (i.e., ocean memory; Figure 2a; Figures S4a, S5a, and S6a in Supporting Information S1). Prominent subsurface oceanic signals manifested as basin-wide increased or decreased anomalies of equatorial warm water volume are evident during the transition phases of ENSO (Figures S4a, S5a, and S6a in Supporting Information S1). The recharge-discharge process describing the slow ocean adjustment to ENSO-associated atmospheric circulation anomalies is of central importance to the oscillatory nature of the ENSO phenomenon (Jin, 1997a, 1997b; Meinen & McPhaden, 2000). A similar ocean phase transition process is very weak for the QD variability (Figures 2a and 2b). The equatorial SST and SSH evolutions are largely simultaneous at the QD timescale, as also shown by their Hovmöller diagrams with multiple SSH products (Figure S8 in Supporting Information S1). It appears that equatorial ocean dynamics are inadequate to provide sufficient ocean memory for the existence of an ENSO-like oscillatory mode in the tropical Pacific on decadal timescales (Z. Liu, 2002). Moreover, an oceanic Rossby wave signal in the subtropical North Pacific at the initial phase is manifested as a negative SSH anomaly (Figure 2a), which indicates that it is not a positive precursor for the following positive phase (Figures 2b–2e). By broadening the meridional data range used in the analysis, we also assess possible positive SSH precursors from the subtropical South Pacific (Figures S9a and S10 in Supporting Information S1) and notice no clear extratropical propagational evidence for the subsequent positive QD phase (Figure S9e in Supporting Information S1). These results suggest that the QD variability might largely reflect reddening ocean processes instead of being a physical oscillatory mode.

4. Physical Processes and Dynamical Origin of Tropical Pacific QD Variability

Next, we conduct an ocean mixed-layer heat budget analysis over the Niño4 region to examine the detailed physical processes governing the corresponding SST variability. The heat budget closure is reasonably good throughout the study period (Figure S11 in Supporting Information S1). To examine the driving processes of SST variability on QD timescales, Figure 3 displays the cross-regression coefficients between the different physical feedbacks, as well as their combinations, and QD SST variability. The time tendency term (dT/dt; Figure 3a) is relatively small compared to the main feedback terms and thus the decadal variability can be regarded at a quasi-equilibrium state to first order. As shown in Figure 3b, both the thermal damping (td) by anomalous net surface heat flux and the dynamical damping (dd) by the mean ocean circulation act to damp the local SST anomalies, with the former playing the dominant role. A further decomposition shows that thermal damping (td) is mainly contributed by the shortwave radiative feedback (sw; Figure S12 in Supporting Information S1). Here, the decomposition is based on the ERA5 reanalysis data set from 1979 to 2018, which exhibits almost identical variability with the net surface heat flux anomalies obtained from GECCO3. As the center of QD SST variability is located close to the edge of the Indo-Pacific warm pool, they can easily trigger anomalous deep convection that can dampen the initial SST warming by reducing solar insolation. In contrast, the thermocline feedback (Figure 3c) and anomalous ocean currents that act on mean temperature gradients (Figure 3d), are major positive feedbacks contributing to SST anomaly growth. In particular, there is a convergent ocean surface current toward the Niño4 region that can transport the climatological warm temperature via horizontal advection (Figures S13aand S13b in Supporting Information S1). The consequent local anomalous downward motions reduce the cooling effects of the mean upwelling and thus increase SST anomalies (Figure S13c in Supporting Information S1). In addition, surface westerly winds to the west of the central Pacific warm SST anomalies lead to a deepening of the local thermocline and fuel the development of the surface warming via the thermocline feedback. We emphasize that all these positive feedbacks are largely in phase with the SST anomaly evolution with a minor phase lag, which cannot provide enough memory to sustain a linear oscillatory regime (Figures 3c and 3d).

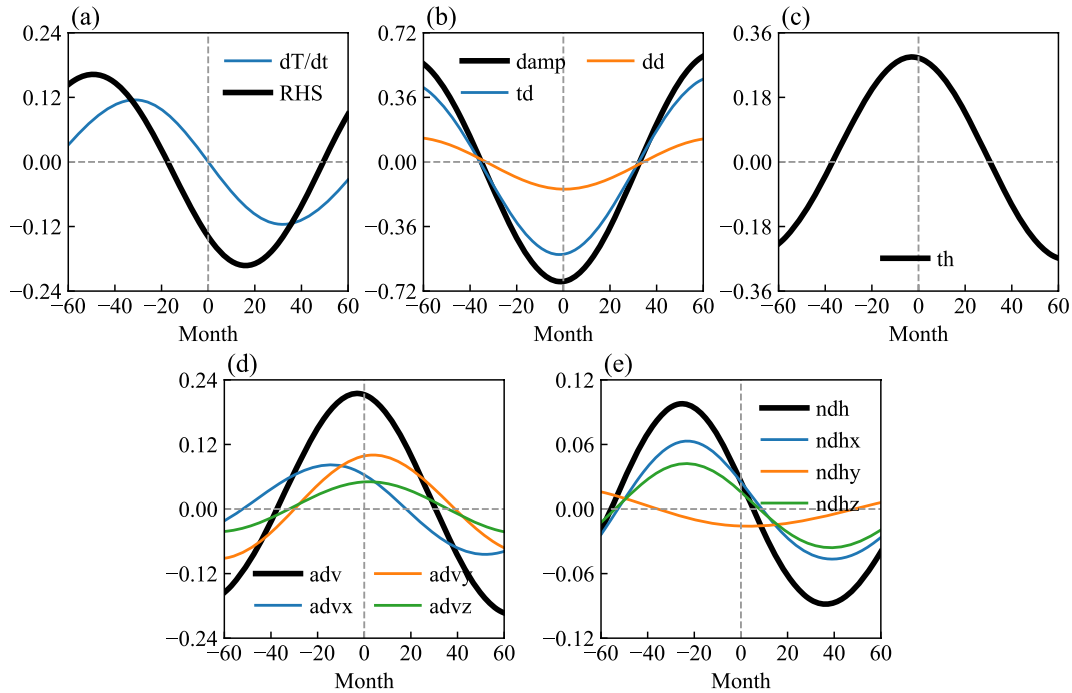


Figure 3. Cross regression coefficients of different feedbacks (°C/year) for the normalized mixed layer temperature in the Niño4 region on quasi-decadal (QD) timescales (8–20 yr bandpass filtered). Positive *x*-axis values (unit: month) indicate feedbacks lag the ocean temperature and negative *x*-axis values indicate they lead. The tendency term is denoted by "dT/dt", which can be decomposed into damping feedback (damp), thermocline feedback (th), advective feedbacks (adv), and nonlinear dynamical heating (ndh). The damping feedback consists of thermal damping (td) and dynamical damping (dd). The "*x*", "*y*", and "*z*" suffixes in (d and e) represent the corresponding zonal, meridional, and vertical components, respectively. The abbreviation "RHS" denotes the summation of all the feedbacks on the right-hand side of Equation 1.

Interestingly, there is a conspicuous phase-lag relationship between the NDH term and QD variability (Figure 3e), providing a potential origin for the QD variability. To gain more insights into the NDH's role, Figure 4 displays the NDH time-series, its connections with the ENSO nonlinearity, and comparisons with the QD SST variability. Only interannual components (<8 yr) are used in calculating the nonlinear quadratic terms to avoid possible interference from the decadal variability. The NDH variability is highly consistent among different data sets (Figure S14 in Supporting Information S1) and dominated by its zonal component (Figure S15 in Supporting Information S1). It is equal to the sum of quadratic products between ENSO-related ocean fields (Figures S16 and S17a in Supporting Information S1) and can be roughly represented by the magnitude squared of ENSO intensity (i.e $(\text{Niño3.4})^2$; Figure 4a). In particular, the NDH and ENSO magnitude squared tend to be large during strong El Niño events (e.g., 1972, 1982, 1997, 2009, 2015), which generally match the phase transition of the QDV from positive phase to negative phase (red dots in Figures 4a and 4b). The close relationship between the QD variability and ENSO nonlinearity is also evidenced by their temporal cross-correlations (Figure S17b in Supporting Information S1). We emphasize that the decadal NDH and the QDV phase transition are not well-matched for the 2015 case, which is possibly due to the edge effect in the filtered data and/or interference from other processes. Figure 4c shows the spatial pattern of cross-regression coefficients between the decadal NDH and QD variability. The QD variability is significantly preconditioned by the NDH over the central equatorial Pacific at a lead of around 30 months, resembling the ENSO-induced NDH on interannual timescales (Figure 4d). This negative NDH could be subsequently amplified by the tropical air-sea interaction processes and eventually evolve into the CP-ENSO-like pattern.

To gain more insight into the preferred periodicity, we display the wavelet results of the NDH and ENSO amplitude squared (Figures 4e and 4f). Their wavelet features are generally similar, both of which exhibit enhanced variance around the strong El Niño events. On the QD timescales, the ENSO amplitude squared shows enhanced power since the 1970s, which resembles the wavelet features of the tropical Niño4 index (Figure 1f). Similar decadal signatures can also be seen from the wavelet results of the mixed-layer NDH, albeit with reduced

19448007, 2022, 10, Downloaded from https://agupubs.onlinelibrary.wiley.com/doi/10.1029/2022GL097903 by CochraneChina, Wiley Online Library on [13/11/2026]. See the Terms and Conditions (https://onlinelibrary.wiley.com/terms-and-conditions) on Wiley Online Library for rules of use; OA articles are governed by the applicable Creative Commons License

19448007, 2022, 10, Downloaded from https://agupubs.onlinelibrary.wiley.com/doi/10.1029/2022GL097903 by CochraneChina, Wiley Online Library on [13/11/2026]. See the Terms and Conditions (https://onlinelibrary.wiley.com/terms-and-conditions) on Wiley Online Library for rules of use; OA articles are governed by the applicable Creative Commons License

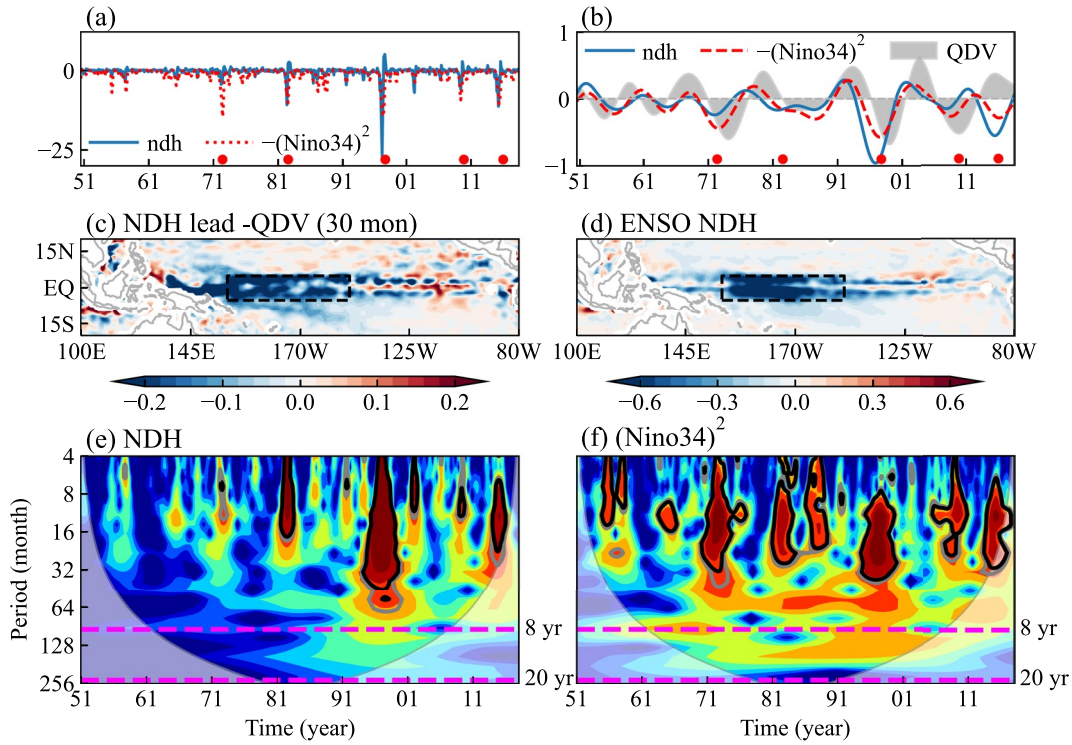


Figure 4. Time series of Niño4 NDH (blue, °C/year) and the sign-reversed ENSO amplitude squared (-(Niño3.4)^2, red). (b) Time series of 8–20 yr bandpass filtered Niño4 index (gray, °C), NDH (blue, °C/year), and ENSO amplitude squared (red). Red dots in (a and b) denote the years of strong El Niño. (c) Regressed 8–20 yr bandpass filtered NDH on QD variability at a lead time of 30 months. The signs of regression coefficients have been reversed. (d) Regressed NDH on the Niño3.4 index. Bias-rectified wavelet power spectra of normalized (e) NDH and (f) ENSO amplitude squared indices. The decadal components have been removed before quadratic analysis. Regions enclosed by gray and black contours indicate statistically significant variability at the 90% and 95% confidence levels when tested against an AR(1) null hypothesis. The parabola regions indicate the "cone of influence", where edge effects become important.

amplitude and time range (Figure 4e). This difference may be related to the ocean data quality and the consequent underestimation of NDH during the early stage. Anomalies of physical quantities in the equatorial subsurface are larger and less affected by other processes compared to those in the mixed layer (Hayashi et al., 2020). Thus, the related subsurface NDH exhibit more prominent decadal variance (Figure S18 in Supporting Information S1). The above result suggests that the quadratic ENSO nonlinearity could lead to the preferred QD timescale. More physically, strong El Niño events generally lead to QDV phase transition and with a return period around 10 yr from 1970 to 2018 (5 cases in 49 yr), which can explain the observed dominant QD periodicity.

5. Conclusions and Discussion

The observations over the past seven decades exhibit prominent QD SST variability in the tropical Pacific that resembles the CP ENSO spatial pattern. Using multiple statistical approaches and data sets, we demonstrate that the observed QD signal is equatorially originated, with the first appearance in the central equatorial Pacific and subsequently spread toward the extratropical regions, in agreement with a previous study (Stuecker, 2018). Further analysis shows that QD variability lacks apparent upper-ocean memory while the ENSO-induced nonlinear rectification effect is a very possible candidate for its dynamical origin. We emphasize that other possible positive feedbacks (i.e., ocean linear dynamics and WES feedbacks) can further enhance QD variance and the CP-ENSO-like SST pattern.

So far, some ocean reanalysis products are still struggling in depicting the ENSO-related upper ocean current correctly (Figure S19 in Supporting Information S1). For example, the ocean reanalysis product from Global Ocean Data Assimilation System (GODAS; Behringer & Xue, 2004; not used in our analyses) has a large bias in upper ocean currents even for the climatology (Huang et al., 2010) and thus fails to capture the anomalous

19448007, 2022, 10, Downloaded from https://agupubs.onlinelibrary.wiley.com/doi/10.1029/2022GL097903 by CochraneChina, Wiley Online Library on [13/11/2026]. See the Terms and Conditions (https://onlinelibrary.wiley.com/terms-and-conditions) on Wiley Online Library for rules of use; OA articles are governed by the applicable Creative Commons License

eastward zonal current in the equatorial central Pacific associated with El Niño events (Figure S19e in Supporting Information S1). A similar problem also exists in the SODA3.3.1 data (Figure S19d in Supporting Information S1; Carton et al., 2018), which may explain its relatively weak NDH intensity (Figure S14c in Supporting Information S1). In this sense, the inaccurate representation of ENSO-related ocean physical quantities can affect the decadal variability of NDH and its connections with QD variability. At present, the ENSO-related NDH is poorly simulated in most of the climate models (Hayashi et al., 2020), presumably leading to unrealistic tropical Pacific decadal variability and their climate impacts. Understanding the causes of those simulation biases is beneficial to improving the model representation of tropical Pacific decadal variability, which we will investigate in future studies.

Data Availability Statement

Reanalysis data sets used in this article are all publicly available: the ERSST at https://psl.noaa.gov/data/gridded/data.noaa.ersst.v5.html; the Hadley Centre SST at https://www.metoffice.gov.uk/hadobs/hadisst/data/HadISST_sst.nc.gz; the Cobe SST at ftp://ftp.cdc.noaa.gov/Datasets/COBE/sst.mon.mean.nc; the Kaplan SST at ftp://ftp.cdc.noaa.gov/Datasets/kaplan_sst/sst.mon.anom.nc; the GECCO3 at https://www.cen.uni-hamburg.de/en/icdc/data/ocean/reanalysis-ocean/gecco3.html; the ORAS5 at https://www.cen.uni-hamburg.de/icdc/data/ocean/easy-init-ocean/ecmwf-oras5.html; the ORAS4 at https://icdc.cen.uni-hamburg.de/thredds/aggregationOras4Catalog.html; the SODA3.3.1 at https://www2.atmos.umd.edu/~ocean/index_files/soda3.3.1_mn_download.htm; the GODAS at https://psl.noaa.gov/data/gridded/data.godas.html; the ERA5 at https://cds.climate.copernicus.eu/#!/search?text=ERA5&type=dataset.

Acknowledgments

The authors would like to thank the editor Suzana J. Camargo and two anonymous reviewers for their time and valuable remarks. The authors also thank Prof. Peng Liu, Dr. Aoyun Xue, Han-Ching Chen, and Sen Zhao for their comments during the early stages of this work. This work was supported by the National Nature Science Foundation of China (42088101, 42125501), and the second Tibetan Plateau Scientific Expedition and Research program (2019QZKK0105). Chao Liu was supported by the Innovation Project of Jiangsu Province (KYCX20_0913), and the China Scholarship Council (File 201908320495). F. F. J. was supported by the U.S. National Science Foundation (AGS-1813611) and Department of Energy (DE-SC0005110). MFS was supported by NOAA's Climate Program Office's Modeling, Analysis, Predictions, and Projections (MAPP) program grant NA20OAR4310445. This is IPRC publication 1567 and SOEST contribution 11516.

References

An, S.-I., & Jin, F.-F. (2004). Nonlinearity and asymmetry of ENSO. *Journal of Climate*, *17*(12), 2399–2412. https://doi.org/10.1175/1520-0442(2004)017<2399:NAAOE>2.0.CO;2

An, S.-I., Jin, F.-F., & Kang, I.-S. (1999). The role of zonal advection feedback in phase transition and growth of ENSO in the Cane-Zebiak model. *Journal of the Meteorological Society of Japan. Series II*, *77*(6), 1151–1160. https://doi.org/10.2151/jmsj1965.77.6_1151

Balmaseda, M. A., Mogensen, K., & Weaver, A. T. (2012). Evaluation of the ECMWF ocean reanalysis system ORAS4. *Quarterly Journal of the Royal Meteorological Society*, *139*(674), 1132–1161. https://doi.org/10.1002/qj.2063

Behringer, D., & Xue, Y. (2004). Evaluation of the global ocean data assimilation system at NCEP: The Pacific Ocean. Paper presented at Eighth Symposium on Integrated Observing and Assimilation Systems for Atmosphere, Ocean, and Land Surface, American Meteorological Society 84th Annual Meeting, American Meteorological Society, Seattle, WA.

Bjerknes, J. (1969). Atmospheric teleconnections from the equatorial Pacific. *Monthly Weather Review*, *97*(3), 163–172. https://doi.org/10.1175/1520-0493(1969)097<0163:ATFTEP>2.3.CO;2

Brassington, G. B. (1997). The modal evolution of the southern oscillation. *Journal of Climate*, *10*(5), 1021–1034. https://doi.org/10.1175/1520-0442(1997)010<1021:TMEOTS>2.0.CO;2

Capotondi, A., Alexander, M. A., Deser, C., & McPhaden, M. J. (2005). Anatomy and decadal evolution of the Pacific subtropical-tropical cells (STCs). *Journal of Climate*, *18*(18), 3739–3758. https://doi.org/10.1175/jcli3496.1

Carton, J. A., Chepurin, G. A., & Chen, L. (2018). SODA3: A new ocean climate reanalysis. *Journal of Climate*, *31*(17), 6967–6983. https://doi.org/10.1175/jcli-d-18-0149.1

Chang, P., Yamagata, T., Schopf, P., Behera, S. K., Carton, J., Kessler, W. S., et al. (2006). Climate fluctuations of tropical coupled systems—The role of ocean dynamics. *Journal of Climate*, *19*(20), 5122–5174. https://doi.org/10.1175/jcli3903.1

Chiang, J. C. H., & Vimont, D. J. (2004). Analogs Pacific and Atlantic meridional modes of tropical atmosphere-ocean variability. *Journal of Climate*, *17*(21), 4143–4158. https://doi.org/10.1175/jcli4953.1

Choi, J., An, S.-I., & Yeh, S.-W. (2011). Decadal amplitude modulation of two types of ENSO and its relationship with the mean state. *Climate Dynamics*, *38*(11–12), 2631–2644. https://doi.org/10.1007/s00382-011-1186-y

Choi, J., An, S.-I., Yeh, S.-W., & Yu, J.-Y. (2013). ENSO-like and ENSO-induced tropical Pacific decadal variability in CGCMs. *Journal of Climate*, *26*(5), 1485–1501. https://doi.org/10.1175/jcli-d-12-00118.1

Chunhan, J., Bin, W., & Jian, L. (2021). Emerging Pacific quasi-decadal oscillation over the past 70 yr. *Geophysical Research Letters*, *48*(2), e2020GL090851. https://doi.org/10.1029/2020gl090851

Clement, A., DiNezio, P., & Deser, C. (2011). Rethinking the ocean's role in the southern oscillation. *Journal of Climate*, *24*(15), 4056–4072. https://doi.org/10.1175/2011jcli3973.1

Di Lorenzo, E., Cobb, K. M., Furtado, J. C., Schneider, N., Anderson, B. T., Bracco, A., et al. (2010). Central Pacific El Niño and decadal climate change in the North Pacific ocean. *Nature Geoscience*, *3*(11), 762–765. https://doi.org/10.1038/ngeo984

Di Lorenzo, E., Schneider, N., Cobb, K. M., Franks, P. J. S., Chhak, K., Miller, A. J., et al. (2008). North Pacific Gyre Oscillation links ocean climate and ecosystem change. *Geophysical Research Letters*, *35*(8), 1–6. https://doi.org/10.1029/2007gl032838

Duchon, C. E. (1979). Lanczos filtering in one and two dimensions. *Journal of Applied Meteorology*, *18*(8), 1016–1022. https://doi.org/10.1175/1520-0450(1979)018<1016:LFIOAT>2.0.CO;2

Frankignoul, C., & Hasselmann, K. (1977). Stochastic climate models. Part II: Application to sea-surface temperature anomalies and thermocline variability. *Tellus*, *29*(4), 289–305. https://doi.org/10.1111/j.2153-3490.1977.tb00740.x

Gu, D., & Philander, S. G. H. (1997). Interdecadal climate fluctuations that depend on exchanges between the tropics and extratropics. *Science*, *275*(5301), 805–807. https://doi.org/10.1126/science.275.5301.805

Hasselmann, K. (1976). Stochastic climate models part I. Theory. *Tellus*, *28*(6), 473–485. https://doi.org/10.1111/j.2153-3490.1976.tb00696.x

Hayashi, M., & Jin, F. (2017). Subsurface nonlinear dynamical heating and ENSO asymmetry. *Geophysical Research Letters*, *44*(24), 12427–12435. https://doi.org/10.1002/2017gl075771

Hayashi, M., Jin, F.-F., & Stuecker, M. F. (2020). Dynamics for El Niño-La Niña asymmetry constrain equatorial-Pacific warming pattern. *Nature Communications*, *11*(1), 4230. https://doi.org/10.1038/s41467-020-17983-y

Hersbach, H., Bell, B., Berrisford, P., Hirahara, S., Horányi, A., Muñoz-Sabater, J., et al. (2020). The ERA5 global reanalysis. *Quarterly Journal of the Royal Meteorological Society*, *146*(146), 1999–2049. https://doi.org/10.1002/qj.3803

Huang, B., Thorne, P. W., Banzon, V. F., Boyer, T., Chepurin, G., Lawrimore, J. H., et al. (2017). Extended reconstructed sea surface temperature, Version 5 (ERSSTv5): Upgrades, validations, and intercomparisons. *Journal of Climate*, *30*(20), 8179–8205. https://doi.org/10.1175/jcli-d-16-0836.1

Huang, B., Xue, Y., Zhang, D., Kumar, A., & McPhaden, M. J. (2010). The NCEP GODAS ocean analysis of the tropical Pacific mixed layer heat budget on seasonal to interannual time scales. *Journal of Climate*, *23*(18), 4901–4925. https://doi.org/10.1175/2010jcli3373.1

Ishii, M., Shouji, A., Sugimoto, S., & Matsumoto, T. (2005). Objective analyses of sea-surface temperature and marine meteorological variables for the 20th century using ICOADS and the Kobe Collection. *International Journal of Climatology*, *25*(7), 865–879. https://doi.org/10.1002/joc.1169

Jin, F.-F. (1997a). An equatorial ocean recharge paradigm for ENSO. Part I: Conceptual model. *Journal of the Atmospheric Sciences*, *54*(7), 811–829. https://doi.org/10.1175/1520-0469(1997)054<0811:AEORPF>2.0.CO;2

Jin, F.-F. (1997b). An equatorial ocean recharge paradigm for ENSO. Part II: A stripped-down coupled model. *Journal of the Atmospheric Sciences*, *54*(7), 830–847. https://doi.org/10.1175/1520-0469(1997)054<0830:AEORPF>2.0.CO;2

Jin, F.-F. (2001). Low-frequency modes of tropical ocean dynamics. *Journal of Climate*, *14*(18), 3874–3881. https://doi.org/10.1175/1520-0442(2001)014<3874:LFMOTO>2.0.CO;2

Jin, F.-F., An, S.-I., Timmermann, A., & Zhao, J. (2003). Strong El Niño events and nonlinear dynamical heating. *Geophysical Research Letters*, *30*(3), 1120. https://doi.org/10.1029/2002gl016356

Kao, P., Hung, C., & Hong, C.-C. (2018). Increasing influence of central Pacific El Niño on the inter-decadal variation of spring rainfall in northern Taiwan and southern China since 1980. *Atmospheric Science Letters*, *19*(12), e864. https://doi.org/10.1002/asl.864

Kennedy, J. J., Rayner, N. A., Smith, R. O., Parker, D. E., & Saunby, M. (2011). Reassessing biases and other uncertainties in sea surface temperature observations measured in situ since 1850: 1. Measurement and sampling uncertainties. *Journal of Geophysical Research*, *116*(D14), D14103. https://doi.org/10.1029/2010jd015218

Kim, G.-I., & Kug, J.-S. (2020). Tropical Pacific decadal variability induced by nonlinear rectification of El Niño-Southern Oscillation. *Journal of Climate*, *33*(17), 7289–7302. https://doi.org/10.1175/jcli-d-19-0123.1

Kleeman, R., McCreary, J. P., & Klinger, B. A. (1999). A mechanism for generating ENSO decadal variability. *Geophysical Research Letters*, *26*(12), 1743–1746. https://doi.org/10.1029/1999gl900352

Köhl, A. (2020). Evaluating the GECCO3 1948–2018 ocean synthesis—A configuration for initializing the MPI-ESM climate model. *Quarterly Journal of the Royal Meteorological Society*, *146*(730), 2250–2273. https://doi.org/10.1002/qj.3790

Liang, X. S., Xu, F., Rong, Y., Zhang, R., Tang, X., & Zhang, F. (2021). El Niño Modoki can be mostly predicted more than 10 yr ahead of time. *Scientific Reports*, *11*(1), 17860. https://doi.org/10.1038/s41598-021-97111-y

Liu, C., Zhang, W., Stuecker, M. F., & Jin, F. (2019). Pacific meridional mode-western North Pacific tropical cyclone linkage explained by tropical Pacific quasi-decadal variability. *Geophysical Research Letters*, *46*(22), 13346–13354. https://doi.org/10.1029/2019gl085340

Liu, Z. (2002). How long is the memory of tropical ocean dynamics? *Journal of Climate*, *15*(23), 3518–3522. https://doi.org/10.1175/1520-0442(2002)015<3518:HLITMO>2.0.CO;2

Liu, Z. (2012). Dynamics of interdecadal climate variability: A historical perspective. *Journal of Climate*, *25*(6), 1963–1995. https://doi.org/10.1175/2011jcli3980.1

Liu, Z., & Di Lorenzo, E. (2018). Mechanisms and predictability of Pacific decadal variability. *Current Climate Change Reports*, *4*(2), 128–144. https://doi.org/10.1007/s40641-018-0090-5

Lohmann, K., & Latif, M. (2005). Tropical Pacific decadal variability and the subtropical-tropical cells. *Journal of Climate*, *18*(23), 5163–5178. https://doi.org/10.1175/jcli3559.1

Luo, J.-J., Masson, S., Behera, S., Delecluse, P., Gualdi, S., Navarra, A., & Yamagata, T. (2003). South Pacific origin of the decadal ENSO-like variation as simulated by a coupled GCM. *Geophysical Research Letters*, *30*(24), 2250. https://doi.org/10.1029/2003gl018649

Luo, J.-J., & Yamagata, T. (2001). Long-term El Niño-Southern Oscillation (ENSO)-like variation with special emphasis on the South Pacific. *Journal of Geophysical Research*, *106*(C10), 22211–22227. https://doi.org/10.1029/2000jc000471

Lyu, K., Zhang, X., Church, J. A., Hu, J., & Yu, J.-Y. (2017). Distinguishing the quasi-decadal and multidecadal sea level and climate variations in the Pacific: Implications for the ENSO-like low-frequency variability. *Journal of Climate*, *30*(13), 5097–5117. https://doi.org/10.1175/jcli-d-17-0004.1

Mann, M. E., & Park, J. (1994). Global-scale modes of surface temperature variability on interannual to century timescales. *Journal of Geophysical Research*, *99*(D12), 25819. https://doi.org/10.1029/94jd02396

Mann, M. E., & Park, J. (1999). Oscillatory spatiotemporal signal detection in climate studies: A multiple-taper spectral domain approach. *Advances in Geophysics*, *41*, 1–131. https://doi.org/10.1016/S0065-2687(08)60026-6

Mann, M. E., Steinman, B. A., Brouillette, D. J., & Miller, S. K. (2021). Multidecadal climate oscillations during the past millennium driven by volcanic forcing. *Science*, *371*(6533), 1014–1019. https://doi.org/10.1126/science.abc5810

Mann, M. E., Steinman, B. A., & Miller, S. K. (2020). Absence of internal multidecadal and interdecadal oscillations in climate model simulations. *Nature Communications*, *11*(1), 49. https://doi.org/10.1038/s41467-019-13823-w

McPhaden, M., Busalacchi, A., & Anderson, D. (2010). A TOGA retrospective. *Oceanography*, *23*(3), 86–103. https://doi.org/10.5670/oceanog.2010.26

Meehl, G. A., Arblaster, J. M., Branstator, G., & van Loon, H. (2008). A coupled air-sea response mechanism to solar forcing in the Pacific region. *Journal of Climate*, *21*(12), 2883–2897. https://doi.org/10.1175/2007jcli1776.1

Meehl, G. A., Arblaster, J. M., Matthes, K., Sassi, F., & van Loon, H. (2009). Amplifying the Pacific climate system response to a small 11 yr solar cycle forcing. *Science*, *325*(5944), 1114–1118. https://doi.org/10.1126/science.1172872

Meehl, G. A., Richter, J. H., Teng, H., Capotondi, A., Cobb, K., Doblas-Reyes, F., et al. (2021). Initialized Earth system prediction from subseasonal to decadal timescales. *Nature Reviews Earth & Environment*, *2*(5), 340–357. https://doi.org/10.1038/s43017-021-00155-x

Meinen, C. S., & McPhaden, M. J. (2000). Observations of warm water volume changes in the equatorial Pacific and their relationship to El Niño and La Niña. *Journal of Climate*, *13*(20), 3551–3559. https://doi.org/10.1175/1520-0442(2000)013<3551:OOWWVC>2.0.CO;2

Neelin, J. D., Battisti, D. S., Hirst, A. C., Jin, F.-F., Wakata, Y., Yamagata, T., & Zebiak, S. E. (1998). ENSO theory. *Journal of Geophysical Research*, *103*(C7), 14261–14290. https://doi.org/10.1029/97jc03424

19448007, 2022, 10, Downloaded from https://agupubs.onlinelibrary.wiley.com/doi/10.1029/2022GL097903 by CochraneChina, Wiley Online Library on [13/11/2026]. See the Terms and Conditions (https://onlinelibrary.wiley.com/terms-and-conditions) on Wiley Online Library for rules of use; OA articles are governed by the applicable Creative Commons License

Newman, M., Alexander, M. A., Ault, T. R., Cobb, K. M., Deser, C., Di Lorenzo, E., et al. (2016). The Pacific decadal oscillation, revisited. *Journal of Climate*, *29*(12), 4399–4427. https://doi.org/10.1175/jcli-d-15-0508.1

Nonaka, M., Xie, S.-P., & McCreary, J. P. (2002). Decadal variations in the subtropical cells and equatorial pacific SST. *Geophysical Research Letters*, *29*(7). https://doi.org/10.1029/2001gl013717

Ogata, T., Xie, S.-P., Wittenberg, A., & Sun, D.-Z. (2013). Interdecadal amplitude modulation of El Niño-Southern Oscillation and its impact on tropical Pacific decadal variability. *Journal of Climate*, *26*(18), 7280–7297. https://doi.org/10.1175/jcli-d-12-00415.1

Power, S., Casey, T., Folland, C., Colman, A., & Mehta, V. (1999). Inter-decadal modulation of the impact of ENSO on Australia. *Climate Dynamics*, *15*(5), 319–324. https://doi.org/10.1007/s003820050284

Power, S., Lengaigne, M., Capotondi, A., Khodri, M., Vialard, J., Jebri, B., et al. (2021). Decadal climate variability in the tropical Pacific: Characteristics, causes, predictability, and prospects. *Science*, *374*(6563). https://doi.org/10.1126/science.aay9165

Rayner, N. A., Parker, D. E., Horton, E. B., Folland, C. K., Alexander, L. V., Rowell, D. P., et al. (2003). Global analyses of sea surface temperature, sea ice, and night marine air temperature since the late nineteenth century. *Journal of Geophysical Research*, *108*(D14). https://doi.org/10.1029/2002jd002670

Ren, H.-L., Jin, F.-F. F., Stuecker, M., & Xie, R. (2013). ENSO regime change since the late 1970s as manifested by two types of ENSO. *Journal of the Meteorological Society of Japan. Series II*, *91*(6), 835–842. https://doi.org/10.2151/jmsj.2013-608

Rodgers, K. B., Friederichs, P., & Latif, M. (2004). Tropical Pacific decadal variability and its relation to decadal modulations of ENSO. *Journal of Climate*, *17*(19), 3761–3774. https://doi.org/10.1175/1520-0442(2004)017<3761:TPDVAI>2.0.CO;2

Schneider, N., Miller, A. J., Alexander, M. A., & Deser, C. (1999). Subduction of decadal North Pacific temperature anomalies: Observations and dynamics. *Journal of Physical Oceanography*, *29*(5), 1056–1070. https://doi.org/10.1175/1520-0485(1999)029<1056:sodnpt>2.0.co;2

Stuecker, M. F. (2018). Revisiting the Pacific meridional mode. *Scientific Reports*, *8*(1), 3216. https://doi.org/10.1038/s41598-018-21537-0

Stuecker, M. F., Timmermann, A., Jin, F.-F., Proistosescu, C., Kang, S. M., Kim, D., et al. (2020). Strong remote control of future equatorial warming by off-equatorial forcing. *Nature Climate Change*, *10*(2), 124–129. https://doi.org/10.1038/s41558-019-0667-6

Suarez, M. J., & Schopf, P. S. (1988). A delayed action oscillator for ENSO. *Journal of the Atmospheric Sciences*, *45*(21), 3283–3287. https://doi.org/10.1175/1520-0469(1988)045<3283:adaofe>2.0.co;2

Sullivan, A., Luo, J.-J., Hirst, A. C., Bi, D., Cai, W., & He, J. (2016). Robust contribution of decadal anomalies to the frequency of central-Pacific El Niño. *Scientific Reports*, *6*(1), 38540. https://doi.org/10.1038/srep38540

Sun, D.-Z., Zhang, T., Sun, Y., & Yu, Y. (2014). Rectification of El Niño-Southern Oscillation into climate anomalies of decadal and longer time scales: Results from forced ocean GCM experiments. *Journal of Climate*, *27*(7), 2545–2561. https://doi.org/10.1175/jcli-d-13-00390.1

Sun, F., & Yu, J.-Y. (2009). A 10–15 yr modulation cycle of ENSO intensity. *Journal of Climate*, *22*(7), 1718–1735. https://doi.org/10.1175/2008jcli2285.1

Tourre, Y. M., Rajagopalan, B., Kushnir, Y., Barlow, M., & White, W. B. (2001). Patterns of coherent decadal and interdecadal climate signals in the Pacific Basin during the 20th century. *Geophysical Research Letters*, *28*(10), 2069–2072. https://doi.org/10.1029/2000gl012780

Wang, S.-Y., Gillies, R. R., Hipps, L. E., & Jin, J. (2011). A transition-phase teleconnection of the Pacific quasi-decadal oscillation. *Climate Dynamics*, *36*(3–4), 681–693. https://doi.org/10.1007/s00382-009-0722-5

Wang, S.-Y., Gillies, R. R., Jin, J., & Hipps, L. E. (2009). Recent rainfall cycle in the Intermountain Region as a quadrature amplitude modulation from the Pacific decadal oscillation. *Geophysical Research Letters*, *36*(2). https://doi.org/10.1029/2008GL036329

Wang, S.-Y., Gillies, R. R., Jin, J., & Hipps, L. E. (2010). Coherence between the Great Salt Lake level and the Pacific quasi-decadal oscillation. *Journal of Climate*, *23*(8), 2161–2177. https://doi.org/10.1175/2009jcli2979.1

Wang, S.-Y., Hakala, K., Gillies, R. R., & Capehart, W. J. (2014). The Pacific quasi-decadal oscillation (QDO): An important precursor toward anticipating major flood events in the Missouri River Basin? *Geophysical Research Letters*, *41*(3), 991–997. https://doi.org/10.1002/2013gl059042

Wang, X., Jin, F.-F., & Wang, Y. (2003a). A tropical ocean recharge mechanism for climate variability. Part I: Equatorial heat content changes induced by the off-equatorial wind. *Journal of Climate*, *16*(22), 3585–3598. https://doi.org/10.1175/1520-0442(2003)016<3585:atormf>2.0.co;2

Wang, X., Jin, F.-F., & Wang, Y. (2003b). A tropical ocean recharge mechanism for climate variability. Part II: A unified theory for decadal and ENSO modes. *Journal of Climate*, *16*(22), 3599–3616. https://doi.org/10.1175/1520-0442(2003)016<3599:atormf>2.0.co;2

White, W. B., & Liu, Z. (2008a). Nonlinear alignment of El Niño to the 11 yr solar cycle. *Geophysical Research Letters*, *35*(19), L19607. https://doi.org/10.1029/2008gl034831

White, W. B., & Liu, Z. (2008b). Resonant excitation of the quasi-decadal oscillation by the 11 yr signal in the Sun's irradiance. *Journal of Geophysical Research*, *113*(C1), C01002. https://doi.org/10.1029/2006jc004057

White, W. B., Tourre, Y. M., Barlow, M., & Dettinger, M. (2003). A delayed action oscillator shared by biennial, interannual, and decadal signals in the Pacific Basin. *Journal of Geophysical Research*, *108*(C3). https://doi.org/10.1029/2002jc001490

Zeller, M., McGregor, S., van Sebille, E., Capotondi, A., & Spence, P. (2020). Subtropical-tropical pathways of spiciness anomalies and their impact on equatorial Pacific temperature. *Climate Dynamics*, *56*(3–4), 1131–1144. https://doi.org/10.1007/s00382-020-05524-8

Zhang, D., & McPhaden, M. J. (2006). Decadal variability of the shallow Pacific meridional overturning circulation: Relation to tropical sea surface temperatures in observations and climate change models. *Ocean Modeling*, *15*(3–4), 250–273. https://doi.org/10.1016/j.ocemod.2005.12.005

Zhao, S., Jin, F., Long, X., & Cane, M. A. (2021). On the breakdown of ENSO's relationship with thermocline depth in the central-equatorial Pacific. *Geophysical Research Letters*, *48*(9), e2020GL092335. https://doi.org/10.1029/2020gl092335

Zuo, H., Balmaseda, M. A., Tietsche, S., Mogensen, K., & Mayer, M. (2019). The ECMWF operational ensemble reanalysis-analysis system for ocean and sea ice: A description of the system and assessment. *Ocean Science*, *15*(3), 779–808. https://doi.org/10.5194/os-15-779-2019

19448007, 2022, 10, Downloaded from https://agupubs.onlinelibrary.wiley.com/doi/10.1029/2022GL097903 by CochraneChina, Wiley Online Library on [13/11/2026]. See the Terms and Conditions (https://onlinelibrary.wiley.com/terms-and-conditions) on Wiley Online Library for rules of use; OA articles are governed by the applicable Creative Commons License